

Jumps in Real-time Financial Markets: A New Nonparametric Test and Jump Clustering

Suzanne S. Lee and Per A. Mykland*

Abstract

We introduce a new nonparametric jump test for continuous-time asset pricing models. It distinguishes actual arrivals of jumps and different jump sizes. Asymptotic distribution of the test statistics is provided, and we demonstrate that it is desirable to use high-frequency data. We explore dynamic jump intensity structure through the test, and find empirical evidence of jump clustering in foreign currency exchange markets. Its implication for financial risk management, in particular value at risk, is also discussed.

*Lee is with the Georgia Institute of Technology, Finance Area. Mykland is with the University of Chicago, Department of Statistics. We would like to thank Federico Bandi, George Constantinides, Pietro Veronesi, and Ruey Tsay for suggestions and comments. Financial support for this research from the National Science Foundation (DMS-02-04-639) and Oscar Mayer Dissertation Fellowships is gratefully acknowledged. Any comments are welcome. Please send any correspondence to: Suzanne S. Lee, phone: 404.894.4963, email: suzanne.lee@mgt.gatech.edu.

Normal financial market evolution is interrupted by completely unexpected incidences such as market crashes, corporate defaults, central bank announcements, and international events. These extreme market uncertainties generate significant discontinuities in financial variables. Empirical evidences of such discontinuities, so called “Jumps” in financial markets, have been well documented in recent literature.¹ Accordingly, the substantial impact of jumps on financial management has also been shown in a number of studies. Applications range from portfolio and risk management to option or bond pricing and hedging.² It has become important to incorporate jumps into continuous-time asset pricing models because they provide reasonable explanations for a number of market phenomena such as the excess kurtosis and skewness of return distributions and the implied volatility smile in option markets. Moreover, it also allows us for the management of a different kind of risk associated with their different hedging demand, in addition to the usual diffusive risk to which market participants are exposed. In order for investors to manage the two types of risk differently, it is critical to distinguish jumps from diffusion for their applications.

The difficulty of disentangling jumps in continuous-time models lies in the fact that we can only observe realized data at discrete times. Therefore, we have to make an econometric inference for jumps in continuous-time models using discrete price changes, some of which may be from the diffusion part, but still yield exactly the same discreteness in data as that which the jump part can provide. Decision making will be affected by incorrectly identified jumps, which have an effect on jump intensity estimation. In addition, classifying jumps can be necessary in terms of their relevance to the application. For instance, intermediate price discreteness, which does not matter for aggressive investors, can matter significantly for passive investors. Furthermore, an investigation of the dynamics of jump arrivals can help forecast future return distributions.³

We propose a new testing device that can solve the problems discussed above in a nonpara-

metric fashion. It disentangles jumps' arrivals and classify jump types in terms of their sizes. The importance of detecting sizes and arrivals lies in dynamic hedging applications among many others: see Naik and Lee (1990), and Bertsimas *et al.* (2001). The impact of jumps becomes more crucial under a larger variance of jumps, especially as jumps increase in size, since hedging error is more likely to go beyond one's tolerance level as a result. In other words, the size of jumps determines the degrees of market incompleteness. Arrival detection becomes important in a dynamic rebalance of a derivative hedging portfolio, as discussed in Collin-Dufresne and Hugonnier (2001) on the temporal resolution of uncertainty.

The advantage of a nonparametric approach is its robustness to model misspecification. There are a few other nonparametric approaches to jumps in the literature. Aït-Sahalia (2002) suggests a diffusion criterion based on transition density to test the presence of jumps. Bandi and Nguyen (2003) and Johannes (2004) provide consistent nonparametric estimators for jump diffusion models based on the kernel estimation method. Barndorff-Nielsen and Shephard (2004) suggest a test to indicate the presence of jumps over a certain time interval by comparing realized power and bipower variation. Their methodology is using two integrated quantities. Because the integrations contain all possible jumps in the interval, they cannot distinguish how many jumps were present within the interval, when in the interval a jump occurs, and how large arrived jump sizes are, although it can still tell its presence. There is increased interest in this problem by other research groups. In particular, a wavelet approach is under development by Fan, Wang, and Xu.

There are a number of different parametric inference methodologies that have been developed and applied in theoretical and empirical studies for jumps in continuous-time asset pricing models. They include Implied State Generalized Method of Moments (IS-GMM): see Pan (2002), Maximum Likelihood Estimation: see Shaumburg (2001), Efficient Method of Moment (EMM): see

Chernov *et al.* (2003), Bayesian approach: Eraker *et al.* (2003), volatility estimation and different types of jumps under Levy processes: see Aït-Sahalia (2003) and Aït-Sahalia and Jacod (2005) . All, however, run the risk of incorrect specification for functionals in their chosen models, which is not the case with our nonparametric test.

Moreover, another merit of our new test is that it is robust to nonstationarity of the processes, which is a common feature of financial variables.

We apply our new test to investigate a time-varying intensity structure in currency exchange markets. With detected jumps, we find supporting evidence that jumps cluster over time in foreign currency exchange markets. This finding on the jump clustering dynamics has an interesting implication for risk management. Specifically, we study how such clustering influences value at risk (VaR) of an underlying exchange rate process and its derivative securities. We illustrate that value at risk (VaR) after an arrival of jump under jump clustering is consistently greater than that under static jump intensity. This is because jump clustering implies a higher jump intensity after an arrival of jump, which makes the tail of future return distribution fatter. This characterizes the consequence of volatile markets after a market jump arrives.

The rest of the paper is organized as follows. Section 1 sets up a theoretical model framework for financial variables to test jumps. It describes the intuition behind our new test, defines the test statistic, and derives its asymptotic distribution to provide a benchmark for tests. A diffusion rejection region can be determined accordingly. We investigate finite sample behavior of the test by presenting the size and power of our new test with simulation. Section 2 presents empirical evidence of jump clustering and its economic implication are discussed in Section 3. Simulation study is in Section 4. Finally, we conclude in Section 5. All the proofs are in Section 6.

1 A Theoretical Model for the Test and Its Asymptotic Theory

We employ a one-dimensional asset return process with a fixed complete probability space $(\Omega, \mathcal{F}_t, \mathcal{P})$ where $\{\mathcal{F}_t : t \in [0, T]\}$ is a right-continuous information filtration for market participants, and \mathcal{P} is a data-generating measure. Let the continuously compounded return be written as $d\log S(t)$ for $t \geq 0$, where $S(t)$ is the asset price at t under \mathcal{P} . We are supposed to test jumps in the asset returns as follows. The null hypothesis of no jumps in the market is represented as

$$d\log S(t) = \mu(t)dt + \sigma(t)dW(t)$$

where $W(t)$ is a \mathcal{F}_t -adapted standard Brownian Motion. The drift $\mu(t)$ and spot volatility $\sigma(t)$ are \mathcal{F}_t -measurable continuous functions, such that the underlying process is a diffusion. Its alternative hypothesis is given by

$$d\log S(t) = \mu(t)dt + \sigma(t)dW(t) + Y(t)dJ(t)$$

where $dJ(t)$ is a jump-counting process with intensity $\lambda(t)$, and $Y(t)$ is the jump size whose mean is $\mu_y(t)$ and standard deviation is $\sigma_y(t)$, which are also \mathcal{F}_t -measurable continuous functions. Observation of $S(t)$, equivalently $\log S(t)$, only occurs at discrete times $0 = t_0 < t_1 < \dots < t_n = T$. For simplicity, this paper assumes observation times are equally spaced: $\Delta t = t_i - t_{i-1}$. This simplified assumption can easily be generalized to nonequidistant cases by letting $\max_i(t_i - t_{i-1}) \rightarrow 0$. We also impose the following necessary assumption on price processes throughout this paper.

Assumption 1

$$\mathbf{A1.1} \quad \sup_i \sup_{t_i \leq u \leq t_{i+1}} |\mu(u) - \mu(t_i)| = O_p(\sqrt{\Delta t})$$

$$\mathbf{A1.2} \quad \sup_i \sup_{t_i \leq u \leq t_{i+1}} |\sigma(u) - \sigma(t_i)| = O_p(\sqrt{\Delta t})$$

Following Pollard (2002), we use O_p notation to mean that for random vectors $\{X_n\}$ and non-negative random variable $\{d_n\}$, $X_n = O_p(d_n)$ if for each $\epsilon > 0$, there exists a finite constant M_ϵ such that $P(|X_n| > M_\epsilon d_n) < \epsilon$ eventually. One can interpret this assumption as the drift and diffusion coefficients do not dramatically changes over any one time interval. This assumption covers most of the models that incorporate jumps in continuous-time asset price processes in finance literature. The drift and diffusion coefficients are allowed to depend on the process itself. It also satisfies the stochastic volatility plus finite activity jump semimartingale class in Barndorff-Nielsen and Shephard (2004) and the reference therein.

1.1 Intuition and Definition of the Nonparametric Jump Test

We address in this subsection the intuition behind our new testing technique and define the jump test statistic, T . When a jump arrives, the realized return is expected to be much higher than that due only to purely continuous random innovations if the observation time interval is short. Because discrete observations from continuous processes with higher variations would also give high realized returns even without jumps, it is natural to standardize the return by a measure that explains the local variation only from the continuous part of the process. We call this measure as local volatility.⁴ This intuition is incorporated into our test. It basically compares a realized return to a consistently estimated local volatility using corresponding local movement of returns. More specifically, the ratio of return to estimated local volatility creates the test statistic for jumps. In order to estimate the variation of a process, we often use a nonparametric integrated variance estimator, that is, the realized power (quadratic) variation defined as the sum of squared returns

$$\text{plim}_{n \rightarrow \infty} \sum_{i=2}^n (\log S(t_i) - \log S(t_{i-1}))^2.$$

This well-known variance estimator is unfortunately inconsistent under the presence of jumps in the return process. Alternatively, the realized bipower variation defined as the sum of products of consecutive absolute returns

$$\text{plim}_{n \rightarrow \infty} \sum_{i=3}^n |\log S(t_i) - \log S(t_{i-1})| |\log S(t_{i-1}) - \log S(t_{i-2})|$$

has been suggested and is shown to be a consistent estimator for the integrated volatility, when there are jumps in return processes: see Barndorff-Nielsen and Shephard (2003) and Aït-Sahalia (2004). Despite the intuition that jumps in the process may change the volatility estimation, it remains consistent, no matter how large or small the jump sizes are mixed with the diffusive part, as long as we have highly frequent observations. Our test is based on this interesting insight. A highly volatile market environment makes the distinguishing of jumps harder. As we increase the frequency of observation, however, infrequent Poisson jumps will be detected by the procedure in the end.

For our analysis using high-frequency data, the drift (of order dt) is mathematically negligible compared to the diffusion (of order \sqrt{dt}) and the jump component (of order 1). In fact, the drift estimates have higher standard errors so that it makes the precision of variance estimates decrease if included in variance estimation. Hence, we first study a simplified version of the model without the drift term, i.e., $\mu = 0$, and later, we show that the main result continues to hold with the nonzero drift term. A modified statistic T_μ for the nonzero drift case will be defined, and a corresponding theorem will be presented in subsection 1.5.

For now, we describe the formulation of the statistic, and provide its mathematical definition. Suppose we are interested in a fixed time horizon T , and n is the number of observation during $[0, T]$. Hence, $\Delta t = \frac{T}{n}$. Consider a local movement of the process within a window size K . With returns in the window consisting of K observations, the time-varying local volatility can be

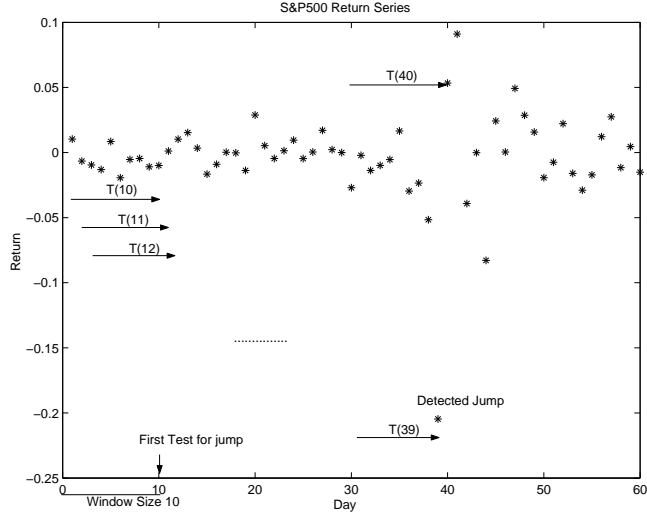


Figure 1: Formation of our new test with a window size $K = 10$

estimated based on the realized bipower variation. The ratio of the next realized return to the estimated local volatility enables us to determine whether there was a jump and how large the jump size was when compared to the local volatility. Figure 1 illustrates the construction of the test. Mathematical notation of the test statistics is as follows.

Definition 1 *The statistic $T(t_i)$ which tests at time t_i whether there was a jump from t_{i-1} to t_i is defined as*

$$T(t_i) = \frac{\log S(t_i) - \log S(t_{i-1})}{\sqrt{\frac{1}{K-2} \sum_{j=i-K+2}^{i-1} |\log S(t_j) - \log S(t_{j-1})| |\log S(t_{j-1}) - \log S(t_{j-2})|}}$$

Notice that the notion of the realized bipower variation is used in the local volatility estimation for the denominator of the statistic. We choose the window size K in such a way that the effect of jumps on the volatility estimation disappears. In the following subsections, we show that T asymptotically follows a normal distribution under the null hypothesis, and it suggests a criterion

to reject the diffusion model based on this asymptotic distribution.

1.2 Under the Absence of Jumps

Suppose our null hypothesis is given by a scalar diffusion process without a drift as

$$d\log S(t) = \sigma(t)dW(t).$$

The asymptotic null distribution of the jump test statistic T is provided in the following Theorem 1. A diffusion rejection region for relevant jumps can be determined by this null distribution.

Theorem 1 *Let $T(t_i)$ be as in Definition 1 under the null and $K = O_p(\Delta t^\alpha)$ where $-1 < \alpha < -0.5$. Suppose Assumption 1 is satisfied. Then as $\Delta t \rightarrow 0$,*

$$\sup_i |T(t_i) - \hat{T}(t_i)| = O_p(\Delta t^{\frac{3}{2}-\delta+\alpha})$$

where δ is in $0 < \delta < \frac{3}{2} + \alpha$, and

$$\hat{T}(t_i) = \frac{U_i}{c}.$$

Here $U_i = \frac{1}{\sqrt{\Delta t}}(W_{t_i} - W_{t_{i-1}})$ and $c = E|U_i| = \sqrt{2}/\sqrt{\pi} \approx 0.7979$.

Proof of Theorem 1: See Appendix 6.2.

In particular, U_i is a standard normal random variable, hence $\hat{T}(t_i)$ follows a normal distribution with mean 0 and variance $\frac{1}{c^2}$. Therefore, our jump test statistic $T(t_i)$ approximately follows the same distribution of $\hat{T}(t_i)$.

1.3 Under the Presence of Jumps

We show in this subsection what happens to the jump test under the alternative hypothesis and discuss the choice of window size and its impact on the test statistic. As mentioned earlier, the

alternative hypothesis is set by a scalar jump diffusion, which describes the presence of jumps in addition to the diffusive market innovation as

$$d\log S(t) = \sigma(t)dW(t) + Y(t)dJ(t).$$

Theorem 2 demonstrates how our test can distinguish jumps. It specifically shows that as the sampling interval Δt goes to 0, the test statistic becomes so large that we can reject the null hypothesis, concluding that there was a jump.

Theorem 2 *Let $T(t_i)$ be as in Definition 1 under the alternative. If $K = O_p(\Delta t^\alpha)$ where $-1 < \alpha < -0.5$, then*

$$T(t_i) \approx \frac{U_i}{c} + \frac{Y(\tau)}{c\sigma\sqrt{\Delta t}} I_{\tau \in (t_{i-1}, t_i]}$$

and $T(t_i) \rightarrow \infty$ as Δt goes to 0.

Proof of Theorem 2: *See Appendix 6.3.*

The benefit of the bipower variation as a local volatility estimator in the denominator of the statistic is that the presence of jumps doesn't affect the consistency of volatility estimation. To retain this benefit, the window size K has to be large enough, but obviously smaller than the number of observations n , so that the effect of jumps in return on estimating local volatility disappears. The condition $K = O_p(\Delta t^\alpha)$ with $-1 < \alpha < -0.5$ satisfies this requirement. Therefore, the choice of sampling frequency Δt will determine the window size. For example, if daily data are used in the analysis, $\Delta t = \frac{1}{252}$, and $K = \beta \Delta t^\alpha$ with $\beta = 1$, integers between 15.87 and 252 are within the required range. The Simulation study in subsection 4.2 finds that if K is within the range, increasing K only elevates the computational burden without large marginal contribution. Hence, the smallest integer K that satisfies the necessary condition would be an optimal choice

of K . In this example, $K^{opt} = 16$, i.e. the local volatility estimation is based on observations of about three weeks just prior to the test if we use daily data.

1.4 Selection of Rejection Region \mathcal{R} and Relation to Jump Sizes

In this subsection, we address how to select rejection region for our proposed test. In effect, we demonstrate that the suggested rejection region allows econometricians to be able to distinguish jumps more precisely as we increase the frequency of observations.

Before we state the criterion, we first discuss the main intuition behind the procedure. As illustrated in Theorem 1 and 2, our test statistics present completely different limiting behavior depending on the presence of jumps. Accordingly, we start to understand how the *maximum* of our test statistics would behave when there is no jumps. This would clearly differentiate observations from null or alternative hypotheses. The way we attack this problem is to find the asymptotic distribution of maximum possible values of statistics when there is no jumps. Such a distribution can then guide us to choose the threshold to distinguish the presence of jumps at the particular testing time. Lemma 1 states the limiting distribution of the maximums as follows.

Lemma 1 *If the conditions for $T(t_i)$, K , and c are as in **Theorem 1** under the null, then as $\Delta t \rightarrow 0$,*

$$\frac{\max |T(t_i)| - C_n}{S_n} \rightarrow \xi$$

where ξ has a cumulative distribution function $P(\xi \leq x) = \exp(-e^{-x})$,

$$C_n = \frac{(2\log n)^{1/2}}{c} - \frac{\log \pi + \log(\log n)}{2c(2\log n)^{1/2}} \text{ and } S_n = \frac{1}{c(2\log n)^{1/2}}.$$

Proof of Lemma 1: See Appendix 6.4.

In short, Lemma 1 implies that if our observed test statistics are not even in the regular maximum region, we will achieve very low likelihood that the observation is from the diffusion process without jumps. For instance, let us suppose we have a fixed significance level of 1% for our tests. Then the threshold for $\frac{|T(t_i)| - C_n}{S_n}$ is β^* such that $P(\xi \leq \beta^*) = \exp(-e^{-\beta^*}) = 0.99$. Equivalently, $\beta^* = -\log(-\log(0.99)) = 4.6001$.

We now generalize the above example of a fixed significance level for the test to any significance level α_n that approaches to 0. Alternatively, β_n approaches to ∞ . In Theorem 3, we explicitly show that the probability of our detecting the jump arrivals approaches to 1 and gives its convergence rate at which we can disentangle jump arrivals more precisely.

Theorem 3 *Let β_n be the $(1 - \alpha_n)^{th}$ percentile of the limiting distribution of ξ in Lemma 1 where α_n is the significance level of test. Suppose there are N jumps over time $[0, T]$. Then,*

$$P(\text{We correctly classify all } N \text{ jumps} | N \text{ jumps}) = 1 - \frac{2}{\sqrt{2\pi}} y_n N + o(y_n N).$$

where $y_n = (\beta_n S_n + C_n) c \sigma \sqrt{\Delta t}$. Therefore, as long as $\beta_n \rightarrow \infty$ slower than $\sqrt{n \log n}$,

$$P(\text{We correctly classify all jumps} | N \text{ jumps}) \longrightarrow 1$$

Proof of Theorem 3: See Appendix 6.5.

Corollary 1 *If the jump intensity is λ and time horizon is from 0 to T , then*

$$E(P(\text{We correctly classify all } N \text{ jumps})) = 1 - \frac{2}{\sqrt{2\pi}} y_n \lambda T + o(y_n \lambda T).$$

Theorem 4 also presents a generalized likelihood of our incorrectly claiming jump arrivals that approaches to 0 quickly and the corresponding convergence rate as the significance level α_n be-

come close to 0.

Theorem 4 *Let β_n be as in Theorem 3. Then, as $\Delta t \rightarrow 0$,*

$$P(\text{We incorrectly reject any non-jumps} | N \text{ Jumps}) = \exp(-\beta_n) + o(\exp(-\beta_n)).$$

Therefore, as $\beta_n \rightarrow \infty$,

$$P(\text{We incorrectly reject any non-jumps} | N \text{ Jumps}) \longrightarrow 0$$

Proof of Theorem 4: *See Appendix 6.6.*

Immediate consequence of our finding in previous theorems is on the accuracy of stochastic jump intensity estimators based on our test.

Theorem 5 *If $\hat{\Lambda}$ is the estimator of cumulative jump intensity and Λ^{actual} is the number of actually realized jumps during $[0, T]$, then*

$$P(\hat{\Lambda} \neq \Lambda^{actual}) = \frac{2}{\sqrt{2\pi}} y_n N + \exp(-\beta_n) + \max(\exp(-\beta_n)).$$

1.5 Size and Power of the Test

In this subsection, we examine the size and power of the new test through Monte Carlo simulation to illustrate its effectiveness. Our asymptotic argument in previous sections requires the sampling interval Δt converge to 0. This idealistic requirement cannot be perfectly met in real applications. This subsection investigates how this test would perform in finite samples, which we mostly have for our empirical studies. The main result from this simulation study shows that as we increase the frequency of observation, the precision of our test becomes greater in terms of its size and power. In other words, its size decreases to zero and its power increases to 1 as we use more frequent

observations. For the series generation, we used the Euler-Maruyama Stochastic Differential Equation (SDE) discretization scheme (Kloeden and Platen (1992)), an explicit order 0.5 strong and order 1.0 weak scheme. We discard the burn-in period – first part of the whole series – to avoid the starting value effect. We use the notation $\Delta t = \frac{1}{252 \times d}$ with d as the number of observations per day throughout.

1.5.1 Constant Volatility

We first consider the simplest model in the class with a fixed volatility. Table I presents the size of the test, which is the probability of rejection when there is no jump (type I error). We simulate two constant volatility diffusion processes with fixed spot volatilities at 30% and 60% respectively. A thousand series of returns over 1 year are simulated at several different frequencies from 1 to 288 observations per day – at highest 5-minute observations. Figure 2 includes simulated daily return from this model and real currency exchange rate of returns to show we are implementing our procedure on series that are close to real returns. The significance level for this study is 5%. Table I shows that increasing the frequency of observation reduces the bias and standard error of the size.

Table II lists the power of the test, that is, the probability of rejection when there is a jump. A thousand simulated tests at different frequencies, again from 1 to 288 observations per day, are performed. Arrivals of six different jump sizes are assumed at 300%, 200%, 100%, 50%, 25%, 10% of the given volatility level of 30%. We chose different jump sizes to show that it is harder to detect smaller-sized jumps at low frequency. However, using our technique, as we increase the frequency, we obtain very high detecting power (above 98%) even for very small sized jumps. For instance, From Table II, we can see that when the relative magnitude of jumps are 10% of volatility, econometricians cannot tell the difference between price changes due to volatility part

NOB	Mean at $\sigma = 0.3$ (SE)	Mean at $\sigma = 0.6$ (SE)
1	1.3432e-03 (7.7769e-05)	1.3305e-03 (7.6239e-05)
2	5.8836e-04 (3.4362e-05)	5.3222e-04 (3.3570e-05)
4	2.1926e-04 (1.4432e-05)	2.1209e-04 (1.4790e-05)
12	6.1637e-05 (4.4644e-06)	5.5911e-05 (4.2684e-06)
24	2.3786e-05 (2.0377e-06)	2.5126e-05 (2.0353e-06)
48	7.7591e-06 (8.0217e-07)	8.6768e-06 (8.3965e-07)
96	4.2436e-06 (4.3177e-07)	4.1876e-06 (4.2736e-07)

Table I: The mean and standard error (in parenthesis) of the size of the test when the significance level α is 5%. The null model is a diffusion process with fixed volatilities, σ at 30% and 60%. NOBS denotes the number of observations per day.

and those due to jump part with lower frequency such as daily. On the other hand, with higher frequencies as much as 30-minute, we can tell the difference more than 95%.

1.5.2 Stochastic Volatility

We examine how the test performs differently for stochastic volatility. Following the empirical study on realized variance of foreign currency exchange rates in Barndorff-Nielsen and Shephard (2004), we assume the spot volatility to be a sum of two uncorrelated Cox, Ingersoll and Ross (1985) square root processes. Specifically, the spot volatility process is modeled as a sum of separate solutions of two different stochastic differential equations,

$$d\sigma_s^2(t) = -\theta_s\{\sigma_s^2(t) - \kappa_s\}dt + \omega_s\sigma_s(t)dB(\theta_s t)$$

where B denotes a Brownian Motion, $\theta_s > 0$, and $\kappa_s \geq \omega_s^2/2$ for $s = 1, 2$. For this simulation, we use estimates calibrated by Barndorff-Nielsen and Shephard (2002) with exchange rate data

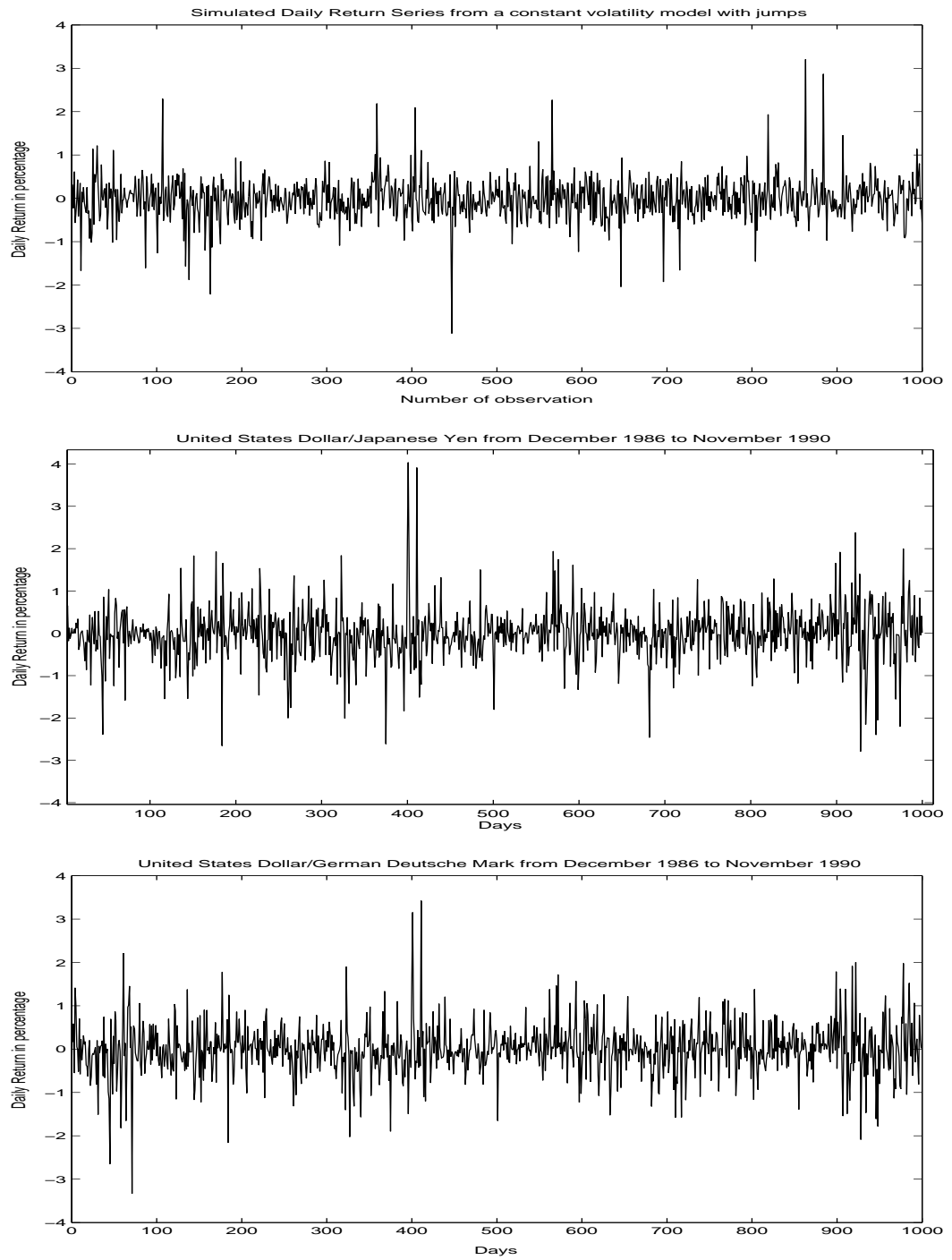


Figure 2: Sample return series simulated from a jump diffusion with constant volatility at 30% and real return of Japanese Yen against United States Dollar and German Mark against United States Dollar

NOBS / y	3	2	1	0.5	0.25	0.1
1	0.9920 (0.0028)	0.9880 (0.0034)	0.9810 (0.0043)	0.9270 (0.0082)	0.4690 (0.0158)	0.0260 (0.0050)
2	0.9860 (0.0037)	0.9840 (0.0040)	0.9800 (0.0044)	0.9730 (0.0051)	0.7380 (0.0139)	0.0570 (0.0073)
4	0.9860 (0.0037)	0.9780 (0.0046)	0.9820 (0.0042)	0.9700 (0.0054)	0.9050 (0.0093)	0.1520 (0.0114)
12	0.9800 (0.0044)	0.9820 (0.0042)	0.9820 (0.0042)	0.9870 (0.0036)	0.9850 (0.0038)	0.5920 (0.0155)
24	0.9950 (0.0022)	0.9860 (0.0037)	0.9890 (0.0033)	0.9890 (0.0033)	0.9770 (0.0047)	0.8880 (0.0100)
48	0.9960 (0.0020)	0.9910 (0.0030)	0.9940 (0.0024)	0.9860 (0.0037)	0.9940 (0.0024)	0.9710 (0.0053)
96	0.9980 (0.0014)	0.9970 (0.0017)	0.9960 (0.0020)	0.9920 (0.0028)	0.9970 (0.0017)	0.9820 (0.0042)

Table II: The mean and standard error (in parenthesis) of power of the test when the significance level α is 5%.

The null model is a diffusion process with fixed volatility σ at 30% and jump size $y \times \sigma$. NOBS denotes the number of observations per day.

in order for our study to mimic the real markets. The values are from

$$E(\sigma_s^2) = p_s 0.509, Var(\sigma_s^2) = p_s 0.461, \text{ for } s = 1, 2$$

with $p_1 = 0.218, p_2 = 0.782, \theta_1 = 0.0429$, and $\theta_2 = 3.74$. We assume no correlation between two Brownian motions in volatility and the random terms in return process, which leaves us with no leverage effect in this study. The distribution of jump size and the Poisson jump counting process are set to be the same as in the case of Constant Volatility. Table III presents again the mean and standard error of the size of the test when the volatility is stochastic. It shows our intuition that if the volatility moves over time, it would be more difficult to disentangle jumps. When we compare Table III to Table I, in every case its bias from the true size of the test (5%) and its standard error with stochastic volatility is greater than those with fixed volatility. We find the same result from the comparison of Table IV and Table II: the power of the test decreases if we have stochastic volatility. This shows that stochastic volatility reduces the precision of jump detection. However, this study does not alter our conclusion in the previous subsection, namely, if we increase the frequency of observation, we can still improve our ability to detect jumps.

2 Dynamics of Jump Arrivals

One of the exclusive advantages of our new test is that it facilitates the investigation of dynamics of jumps. Improvement in empirical option-pricing research with time-varying intensity is stressed in Bates (2002). There are recent empirical studies on jump clustering in individual stock markets using parametric discrete time series models around the market crashes in 1987 (Maheu and McCurdy (2004)). Duffie *et al* (2000) has a theoretical study under an affine jump intensity structure, and Chernov *et al* (1999) take into their consideration a non-affine random jump intensity,

NOB	Mean of size	(SE)
1	3.9110e-03	(1.3319e-04)
2	2.3306e-03	(7.7336e-05)
4	1.3289e-03	(4.3670e-05)
12	4.8131e-04	(1.6731e-05)
24	2.7688e-04	(1.0062e-05)
48	1.4467e-04	(7.2952e-06)
96	8.9449e-05	(4.2818e-06)

Table III: The mean and standard error (in parenthesis) of the size of the test when the significance level α is 5%. The null model is a diffusion process with stochastic volatility. NOBS denotes the number of observations per day.

which can depend on the jump sizes. Jump intensity can be explained by a number of market activities and a correct specification of jump dynamics would be important. Our nonparametric test can provide a simple device to construct a specification since the approach is robust to model misspecification as discussed.

In this section, using our new test, we explore so-called “jump clustering” in foreign currency exchange markets using high frequency data. Jump arrival may lead to a dramatic increase in volatility because market participants react differently after the arrival. Since high volatility can also produce a very large discrepancy in discretely observed security prices, one can question whether a jump leads to another jump or not. Since the new test can dynamically detect the actual arrival of jumps, we can easily provide an answer to the question. We offer the empirical evidence of dynamic structure in jump intensity to explain that the arrival of jumps has a positive impact on future jumps.

Our empirical study is based on the dataset that consists of very high frequency exchange rate of returns up to 5 minutes of German Market per United States Dollar and Japanese Yen

NOB / y	3	2	1	0.5	0.25	0.1
1	0.9470	0.9330	0.8540	0.5720	0.2500	0.0320
	(0.0071)	(0.0079)	(0.0112)	(0.0157)	(0.0137)	(0.0056)
2	0.9730	0.9560	0.9010	0.7270	0.3990	0.0830
	(0.0051)	(0.0065)	(0.0094)	(0.0141)	(0.0155)	(0.0087)
4	0.9770	0.9690	0.9410	0.8480	0.5320	0.1400
	(0.0047)	(0.0055)	(0.0075)	(0.0114)	(0.0158)	(0.0110)
12	0.9790	0.9750	0.9790	0.9360	0.7790	0.3650
	(0.0045)	(0.0049)	(0.0045)	(0.0077)	(0.0131)	(0.0152)
24	0.9870	0.9860	0.9830	0.9610	0.8770	0.5260
	(0.0036)	(0.0037)	(0.0041)	(0.0061)	(0.0104)	(0.0158)
48	0.9880	0.9920	0.9930	0.9880	0.9400	0.6540
	(0.0034)	(0.0028)	(0.0026)	(0.0034)	(0.0075)	(0.0151)
96	0.9970	0.9990	0.9980	0.9920	0.9610	0.8100
	(0.0017)	(0.0010)	(0.0014)	(0.0028)	(0.0061)	(0.0130)

Table IV: The mean and standard error (in parenthesis) of the power of the test when the significance level α is 5%. The null model is a diffusion process with stochastic volatility and the jump size depends on the mean of volatility $\widetilde{\sigma(t)} = E[\sigma(t)]$ with $y \times \widetilde{\sigma(t)}$.

per United States Dollar. The time span is from December 1, 1986 to November 30, 1996. We aggregate 5 minutes to lower frequencies by adding the corresponding returns. We generate data of jump arrivals for our analysis as follows. We set up a diffusion rejection region \mathcal{R} for the test statistic T at a given significance level α and a diffusion rejection function g at time t_i such that

$$g(T(t_i)) = I(T(t_i) \in \mathcal{R}).$$

Thus, detection of jumps over a period can be recorded by a series of this indicator, $g(T(t_i))$, for $i = K, \dots, n$. We then apply a simple autoregressive model of order 1 on this series as

$$g(T(t_i)) = \beta_{u,0} + \beta_{u,1}g(T(t_{i-1})) + \epsilon_i$$

where ϵ_i is a normal error term with mean 0 and a finite variance. u denotes the name of currency that is exchanged to U.S. Dollar, $u = DM, JY$, and $\Delta t = t_i - t_{i-1}$. Because $E[g(T(t_i))] = E[I(T(t_i) \in \mathcal{R})] = \lambda(t_i)$, we can extract the dependence of two successive intensity as

$$\lambda(t_i) = \beta_{u,0} + \beta_{u,1}\lambda(t_{i-1}).$$

Table V and VI shows the significance of positive coefficients $\beta_{u,1}$ that represents the positive impact on future jump arrival of current jump arrival. It increases the intensity of future jumps. We used two different frequencies of 6 hourly and 3 hourly to minimize false jump discovery for both cases. As we decrease the frequency, the effect will eventually disappear. By choosing several different significance levels of tests, we find different coefficients for specific types of jumps.

3 Economic Implication of Jump Cluster for Risk Management

Given the empirical evidence presented in Section 2, we expect to have more jumps with higher intensity in the very near future after an arrival of jump, although the effect will fade out soon.

6 Hourly U.S. Dollar per German Mark Exchange Rate				
α	$\widehat{\beta_{DM,0}}$	95% C.I. ($\widehat{\beta_{DM,0}}$)	$\widehat{\beta_{DM,1}}$	95% C.I. ($\widehat{\beta_{DM,1}}$)
0.1	0.0597	(0.0557,0.0638)	0.0255	(0.0091,0.0418)
0.05	0.0430	(0.0396,0.0464)	0.0204	(0.0040 0.0367)
0.01	0.0244	(0.0218,0.0270)	0.0176	(0.0013,0.0340)
0.005	0.0184	(0.0162,0.0207)	0.0222	(0.0058,0.0385)
0.001	0.0120	(0.0102,0.0138)	0.0166	(0.0002,0.0329)
6 Hourly U.S. Dollar per Japanese Yen Exchange Rate				
α	$\widehat{\beta_{JY,0}}$	95% C.I. ($\widehat{\beta_{JY,0}}$)	$\widehat{\beta_{JY,1}}$	95% C.I. ($\widehat{\beta_{JY,1}}$)
0.1	0.0535	(0.0497,0.0574)	0.0308	(0.0145,0.0472)
0.05	0.0370	(0.0338,0.0402)	0.0320	(0.0157,0.0484)
0.01	0.0197	(0.0173,0.0220)	0.0317	(0.0154,0.0480)
0.005	0.0149	(0.0129,0.0169)	0.0346	(0.0183,0.0510)
0.001	0.0091	(0.0075,0.0107)	0.0488	(0.0325,0.0652)
0.0005	0.0080	(0.0065,0.0095)	0.0340	(0.0177,0.0504)
0.0001	0.0050	(0.0038,0.0061)	0.0484	(0.0320,0.0647)
0.00005	0.004	(0.0029,0.0050)	0.0460	(0.0297,0.0624)

Table V: The parameter estimates for the autoregressive jump arrival model. The significance level of each test is set at $100 \times \alpha\%$, which classifies the detected jump sizes.

3 Hourly U.S. Dollar per German Mark Exchange Rate				
α	$\widehat{\beta_{DM,0}}$	95% C.I. ($\widehat{\beta_{DM,0}}$)	$\widehat{\beta_{DM,1}}$	95% C.I. ($\widehat{\beta_{DM,1}}$)
0.1	0.0495	(0.0469,0.0521)	0.0561	(0.0446,0.0676)
0.05	0.0359	(0.0337,0.0382)	0.0501	(0.0385 0.0616)
0.01	0.0198	(0.0181,0.0214)	0.0294	(0.0179,0.0410)
0.005	0.0164	(0.0150,0.0179)	0.0207	(0.0091,0.0322)
0.001	0.0106	(0.0095,0.0118)	0.0120	(0.0054,0.0235)
3 Hourly U.S. Dollar per Japanese Yen Exchange Rate				
α	$\widehat{\beta_{JY,0}}$	95% C.I. ($\widehat{\beta_{JY,0}}$)	$\widehat{\beta_{JY,1}}$	95% C.I. ($\widehat{\beta_{JY,1}}$)
0.1	0.0497	(0.0470,0.0523)	0.0568	(0.0453,0.0684)
0.05	0.0364	(0.0341,0.0386)	0.0378	(0.0263,0.0493)
0.01	0.0190	(0.0174,0.0206)	0.0220	(0.0105,0.0335)
0.005	0.0152	(0.0138,0.0166)	0.0205	(0.0093,0.0321)
0.001	0.0092	(0.0080,0.0103)	0.0169	(0.0053,0.0284)
0.0005	0.0075	(0.0065,0.0085)	0.0198	(0.0083,0.0313)
0.0001	0.0057	(0.0048,0.0066)	0.0241	(0.0126,0.0357)
0.00005	0.0050	(0.0042,0.0058)	0.0222	(0.0107,0.0338)

Table VI: The parameter estimates for the autoregressive jump arrival model. The significance level of each test is set at $100 \times \alpha\%$, which classifies the detected jump sizes.

This dynamic feature of jump arrivals has an interesting implications for risk management. We discuss in this section how this finding can affect the evaluation of value at risk, denoted as “VaR”.

VaR has been used extensively as a quantitative benchmark to disclose financial risk of banks, security firms or any bundle of their portfolios under a liquid market environment, especially after it was adopted by the U.S. Securities and Exchange Commission (SEC) in the early 1980s. This risk measure is defined as the loss over a given future time horizon s , that is exceeded with a probability p for the given confidence level at $1 - p$. Because it is essentially the p th percentile of future return distribution at time s , it depends critically on its degree of kurtosis, on which jumps would have a strong impact. Choice of s and p can be arbitrary. In practice, for s , a day, a week, or some accounting periods are common choices, and p can be 1% or 5% depending on users’ concern. See Duffie and Pan (1997).

The dynamic jump structure we found implies that the future jump intensity at s is expected to be higher than that under static jump structure. This means we expect to have fatter tails in return distributions at s with dynamic intensity than with static intensity, given that other functionals are the same in the comparison. The fatter tail in the likelihood function makes VaR larger because the p th percentile of the distribution at s with dynamic intensity is lower than that with static one. This follows that jump clustering implies higher VaR. If we find different intensity structures in other applications, our forecast on VaR would be changed accordingly.

We show examples of VaR of exchange rate of Japanese Yen against U.S. Dollar and portfolios of a put option on the rate. In this experiment, we compare cases with a static and dynamic jump intensity. For series generation, we simulate 2000 series from a jump diffusion model of exchange rate of return: one with static and the other with dynamic jump intensity. It is assumed that other functionals are the same under both cases. We set the spot volatility σ at 30%, standard

Daily 99%-VaR	for Underlying Asset A		for In the Money Put Option		for Out of the Money Put Option	
Intensity structure	Static	Dynamic	Static	Dynamic	Static	Dynamic
	1.26	1.31	1.48	1.81	2.23	2.63
Difference(%)	3.97		22.29		17.94	
6 Hour 99%-VaR	for Underlying Asset A		for In the Money Put Option		for Out of the Money Put Option	
Intensity structure	Static	Dynamic	Static	Dynamic	Static	Dynamic
	0.24	0.43	0.38	0.69	0.56	0.94
Difference(%)	79.16		81.57		67.85	
3 Hour 99%-VaR	for Underlying Asset A		for In the Money Put Option		for Out of the Money Put Option	
Intensity structure	Static	Dynamic	Static	Dynamic	Static	Dynamic
	0.12	0.19	0.28	0.66	0.19	0.50
Difference(%)	58.33		135.71		163.15	

Table VII: The examples of 99%-VaR of currency exchange rate and its options. Values of VaR are in percentages. The underlying exchange rate of return process has volatility at 30%, standard deviation of jump size distribution at 60%, fixed jump intensity at 10 per a year. The β_1 coefficient is at 5%.

deviation σ_y at 60%, static jump intensity λ at 10 jumps a year, and the coefficient β_1 for jump clustering at 5%, which we obtain in our empirical study in Section 2. Current exchange rate of Japanese Yen against U.S. Dollar is set at 100, and its future rate is from simulation. Strike rates of put options in the examples are set at 80 and 120 for in the money and out of the money options respectively. Its maturity is set at 1 year. Interest rates in the United States and Japan are set at 2% and 7% respectively. The values for VaR in this exercise are the empirical 99th percentiles of the simulated return distributions.

Table VII illustrates various cases of VaR of exchange rate and its put options at given conditions. This shows that jump clustering consistently yields higher values of VaR for all cases.

4 Monte Carlo Simulation

In this section, we do more Monte Carlo simulation experiments to illustrate the performance of our new test. We address how the test is improved with the frequency of observations. Simulated sample series that consist of various years of observations with different frequencies are considered. Given the finding in Section 1 that stochastic volatility would give similar results, we deal only with the Merton model (1976) with a constant drift, diffusion, and jump intensity. The formulation of the entertained model is

$$d\log S(t) = \mu dt + \sigma dW(t) + Y(t)dJ(t)$$

where λ is the mean number of jumps a year, and $Y(t)$ is the jump size whose distribution is normally distributed with mean μ_y and standard deviation σ_y . The drift μ and mean of jump size distribution μ_y are set at zero in this experiment. The variance of jump sizes compared to volatility level turns out to be the main determinant for telling jumps apart from the diffusions. By choosing several jump size variances, we show how the result can be changed. The value chosen in this study is $\sigma = 30\%$ and $\lambda = 10$ with three different jump size variances, $\sigma_y = 60\%, 30\%, 15\%$, which are selected depending on volatility level σ . Each different case can explain how it performs for different jump sizes.

4.1 Actual Arrival

In order to see how well this test distinguishes actual arrival of jumps, we first consider an total error, $\hat{\Lambda}(T) - \Lambda(T)$ where $\hat{\Lambda}(T)$ denotes the estimate of number of jumps in $[0, T]$ and $\Lambda(T)$ denotes the number of true jumps in $[0, T]$. Then we decompose the total error as

$$\text{Total Error} = \hat{\Lambda}(T) - \Lambda(T) = \hat{\Lambda}(T) - \Lambda^{\text{actual}}(T) + \Lambda^{\text{actual}}(T) - \Lambda(T) = \text{Err}_1 + \text{Err}_2$$

Frequency	Daily	12 hourly	6 hourly	3 hourly	1 hourly
$\sigma = 0.3, \sigma_y = 0.6$	1.00096	0.75078	0.51469	0.40215	0.23383
$\sigma = 0.3, \sigma_y = 0.3$	1.05382	0.77550	0.51883	0.40455	0.23528
$\sigma = 0.3, \sigma_y = 0.15$	1.08480	0.79284	0.53244	0.39956	0.23601

Table VIII: Mean Squared Error 1: $Err_1 = \hat{\Lambda}(T) - \Lambda^{actual}(T)$

and take the first error to be

$$Err_1 = \hat{\Lambda}(T) - \Lambda^{actual}(T)$$

where $\Lambda^{actual}(T)$ denotes the number of actually realized true jumps in discrete observations in $[0, T]$. A smaller first error indicates that we detect arrival of jumps with more accuracy. In Table VIII, we fix $T = 1$ year. It shows the Mean Squared Error 1, $E[Err_1^2]$, with different choices of jump size variances and observation frequencies. As we increase the frequency, the error decreases, and as we decrease the variance of jump sizes, the error increases. Thus, discrete data at low frequency from jumps with low variances do not appear as dramatic changes in return realization; hence, they are less likely to be detected. Given in Table VIII that increasing the frequency increases the precision of detecting realized jumps, we fix in Table IX the frequency at 6 hourly. Then we expanded the terminal horizon T from 1 year to 10 years and note how the results changed. Increasing the horizon decreased the total error as well as the two error components, Err_1 and Err_2 . Therefore, a longer horizon will also increase the precision of jump estimation as well as arrival detection.

4.2 Optimal Window Size K

The optimal choice for window size is studied by simulation in this subsection. We show in plots the relationship between Mean Squared Total Error and the choice of window sizes. In particular,

T	1	3	5	7	10
Total Error	0.73004	0.43436	0.33385	0.27522	0.23589
Error 1	0.51469	0.31870	0.23665	0.20758	0.16871
Error 2	0.21539	0.11567	0.09720	0.06764	0.06718

Table IX: Mean Squared Errors for 6 hourly data with $T = 1, 3, 5, 7, 10$

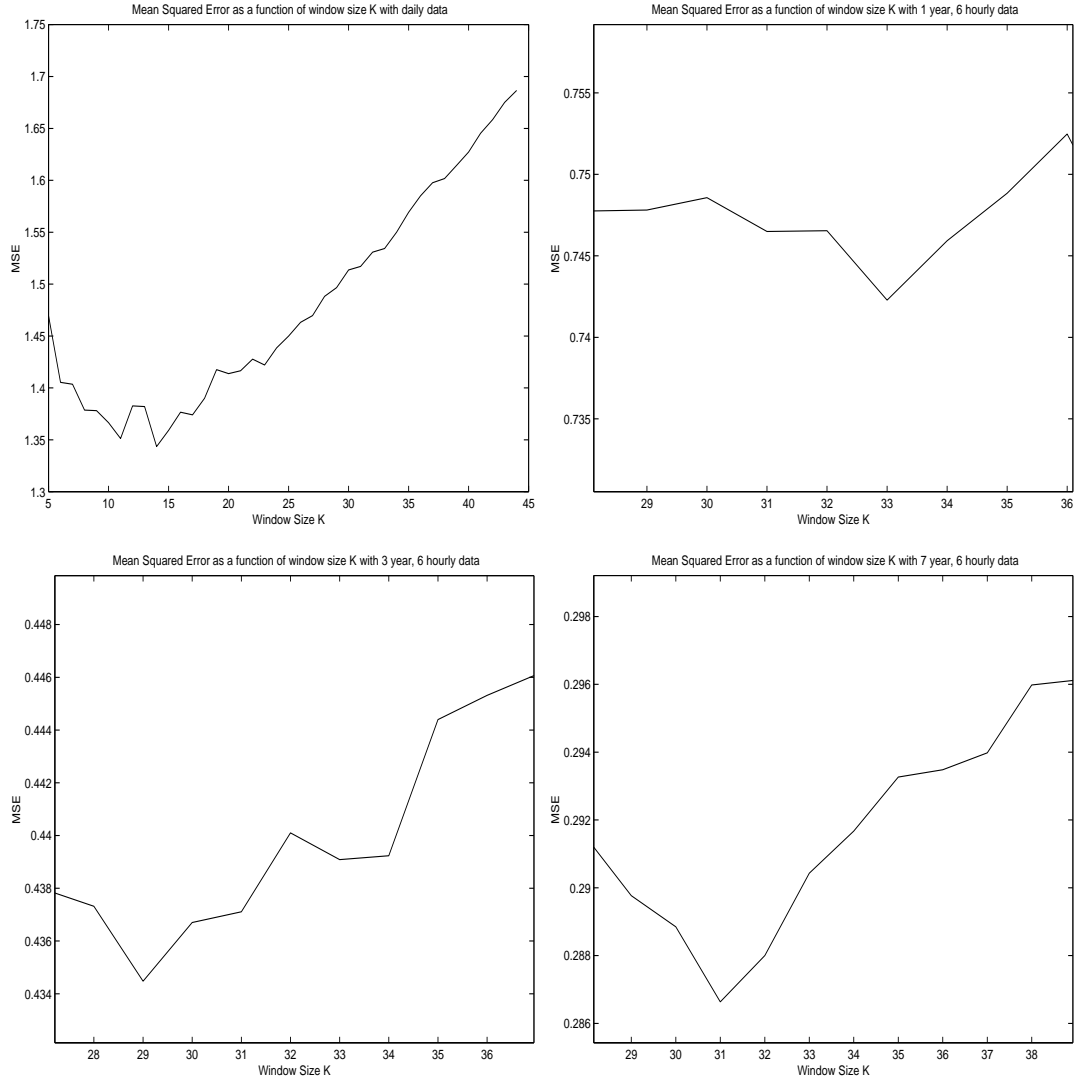


Figure 3: Graphs of Mean Squared Total Error with daily and 6 hourly data as a function of window size K

four cases are plotted in Figure 3 to show optimal choice of window size. The upper left panel shows Mean Squared Total Error as a function of window size K using daily data with the horizon $T = 1$ year. The remaining three use 6 hourly data with the horizon $T = 1, 3$, and 7 years. It turns out that as mentioned in Section 1, it is optimal for K to be the smallest integer in the condition set, $K = O_p(\Delta t^\alpha)$ with $-1 < \alpha < -0.5$, because it gives the lowest Mean Squared Error in our simulation. Increasing window size would not always increase the efficiency of test, especially for the intensity estimation, because it lowers the number of multiple tests if we have a fixed number of observations n .

5 Concluding Remarks

A new nonparametric test is introduced to detect realizations of jumps and classify their magnitudes. Analysts are supposed to determine what they mean by jumps in the first place and choose thresholds accordingly. Overall results from Monte Carlo simulation experiments show that if available, a higher frequency of observations with longer periods can increase the precision of jump tests. Using the new test, we find empirical evidence for jump clustering in foreign currency exchange markets from highly frequent transactions, and illustrate the significance of jump dynamics. We address the implication of jump clustering for value at risk of currency exchange rates and their put options. Jump clustering makes this risk measure consistently greater, which suggests its importance in financial risk management.

6 Appendix

6.1 The Nonzero Drift

The main conclusion of Theorem 1 is not altered under an extension to the nonzero drift case.

Suppose now we have the nonzero drift coefficient $\mu(t)$ for the return process, that is,

$$d\log S(t) = \mu(t)dt + \sigma dW(t).$$

A modified version of Definition 1 for this case is as follows.

Definition 1.1 *The statistic $T_\mu(t_i)$ which tests at time t_i whether there was a jump from t_{i-1} to t_i is defined as*

$$T_\mu(t_i) = \frac{\log S(t_i) - \log S(t_{i-1}) - \hat{m}_i}{\sqrt{\frac{1}{K-2} \sum_{j=i-K+2}^{i-1} |\log S(t_j) - \log S(t_{j-1})| |\log S(t_{j-1}) - \log S(t_{j-2})|}}$$

where

$$\hat{m}_i = \frac{1}{K-1} \sum_{j=i-K+1}^{i-1} (\log S(t_j) - \log S(t_{j-1}))$$

Then we can extend Theorem 1 to the case of nonzero drift as below.

Theorem 1.1 *Let $T_\mu(t_i)$ be as in Definition 1.1 under the null and $K = O_p(\Delta t^\alpha)$ where $-1 < \alpha < -0.5$. Suppose **Assumption 1** is satisfied. Then as $\Delta t \rightarrow 0$,*

$$\sup_i |T_\mu(t_i) - \hat{T}_\mu(t_i)| = O_p(\Delta t^{\frac{3}{2}-\delta+\alpha})$$

where

$$\hat{T}_\mu(t_i) = \frac{U_i - \bar{U}_{i-1}}{c}.$$

Here $\bar{U}_{i-1} = \frac{1}{K-1} \sum_{j=i-K+1}^{i-1} U_j$ and the rest of notations are the same as in **Theorem 1**.

Proof of Theorem 1.1: See Appendix 6.2.

The error rate is the same as the zero drift case since the error due to drift term is dominated by the error due to the diffusion part. $\hat{T}_\mu(t_i)$ asymptotically follows a normal distribution with its mean 0 and variance $\frac{K}{c^2(K-1)} \rightarrow \frac{1}{c^2}$ since $K \rightarrow \infty$. Our choice of K makes the effect of jumps on \hat{m}_i vanish because of the property of the Poisson process for rare jumps, which says that there can be no more than a single jump in an infinitesimal time interval. Because this makes only a finite number, say L , of jumps in the window, the jump test statistic for the nonzero drift case becomes

$$T(t_i) \approx \frac{U_i - \bar{U}_{i-1}}{c} - \frac{L \times Y(\tau)}{c\sigma(K-1)\sqrt{\Delta t}} I_{\tau \in (t_{i-K}, t_{i-1}]}$$

The second term will disappear because of the condition $K\sqrt{\Delta t} \rightarrow \infty$. This shows that jumps in the window have asymptotically negligible effect on testing jumps from t_{i-1} to t_i with our choice of K .

6.2 Proof of Theorem 1 and Theorem 1.1 in Appendix 6.1

For $t_{i-K} < t < t_i$,

$$\log S(t) - \log S(t_{i-K}) = \int_{t_{i-K}}^t \mu(u) du + \int_{t_{i-K}}^t \sigma(u) dW(u).$$

Given the Assumption 1 imposed, we have with A1.1,

$$\begin{aligned} \int_{t_{i-1}}^{t_i} \mu(u) du - \mu(t_{i-1})\Delta t &= O_p(\Delta t^{\frac{3}{2}}) \\ \text{and } \int_{t_{i-K}}^{t_i} \mu(u) du - \mu(t_{i-K})K\Delta t &= O_p(\Delta t^{\frac{3}{2}+\alpha}) \end{aligned}$$

uniformly in all i . This implies

$$\sup_{i, t \leq t_i} \left| \int_{t_{i-K}}^t \{\mu(u) - \mu(t_{i-K})\} du \right| = O_p(\Delta t^{\frac{3}{2}+\alpha})$$

Similarly to *lemma 1* in Mykland and Zhang (2001), under the condition A1.2, we can apply Burkholder's Inequality (Protter (1995)) to get

$$\sup_{i, t \leq t_i} \left| \int_{t_{i-K}}^t \{\sigma(u) - \sigma(t_{i-K})\} dW(u) \right| = O_p(\Delta t^{\frac{3}{2}-\delta+\alpha})$$

where δ can be any number in $0 < \delta < \frac{3}{2} + \alpha$. This result is also uniform in i for the $K = O_p(\Delta t^\alpha)$ as specified. Therefore, over the window, for $t \in [t_{i-K}, t_i]$, $d\log S(t)$ can be approximated by $d\log S^i(t)$ such that

$$d\log S^i(t) = \mu(t_{i-K})dt + \sigma(t_{i-K})dW(t)$$

because

$$\begin{aligned} & |(\log S(t) - \log S(t_{i-K})) - (\log S^i(t) - \log S^i(t_{i-K}))| \\ &= \left| \int_{t_{i-K}}^t (\mu(u) - \mu(t_{i-K})) du + \int_{t_{i-K}}^t (\sigma(u) - \sigma(t_{i-K})) dW(u) \right| = O_p(\Delta t^{\frac{3}{2}-\delta+\alpha}). \end{aligned}$$

For all i, j and $t_j \in [t_{i-K}, t_i]$, the numerator is

$$\begin{aligned} & \log S(t_j) - \log S(t_{j-1}) - \hat{m}_i \\ &= \log S^i(t_j) - \log S^i(t_{j-1}) - \frac{1}{K-1} \sum_{l=i-K+1}^{i-1} (\log S^i(t_l) - \log S^i(t_{l-1})) + O_p(\Delta t^{\frac{3}{2}-\delta+\alpha}) \\ &= \sigma(t_{i-K})W_{\Delta t} - \frac{1}{K-1} \sum_{l=i-K+1}^{i-1} \sigma(t_{i-K})W_{\Delta t} + O_p(\Delta t^{\frac{3}{2}-\delta+\alpha}) \\ &= \sigma(t_{i-K})\sqrt{\Delta t}(U_j - \bar{U}_{i-1}) + O_p(\Delta t^{\frac{3}{2}-\delta+\alpha}) \end{aligned}$$

where $U_j = \frac{1}{\sqrt{\Delta t}}(W_{t_j} - W_{t_{j-1}}) \sim iid \text{ Normal}(0, 1)$, and $\bar{U}_{i-1} = \frac{1}{K-1} \sum_{j=i-K+1}^{i-1} U_j$.

For the denominator, we put a volatility estimator based on the realized bipower variation for integrated volatility estimator: see Barndorff-Nielsen and Shephard(2004). According to *Proposition*

2 in Barndorff-Nielsen and Shephard (2004), the impact of the drift term is negligible; hence, it does not affect the asymptotic limit behavior. Then, we are left to prove the following approximation of scaled volatility estimator.

$$\begin{aligned}\text{plim}_{\Delta t \rightarrow 0} c^2 \hat{\sigma}^2(t) &= \text{plim}_{\Delta t \rightarrow 0} \frac{1}{(K-2)\Delta t} \sum_j |\log S(t_j) - \log S(t_{j-1})| |\log S(t_{j-1}) - \log S(t_{j-2})| \\ &= c^2 \sigma^2(t)\end{aligned}$$

It is due to

$$\begin{aligned}& \frac{1}{(K-2)\Delta t} \sum_{j=i-K+3}^{i-1} |\log S(t_j) - \log S(t_{j-1})| |\log S(t_{j-1}) - \log S(t_{j-2})| \\ &= \frac{1}{(K-2)\Delta t} \sum_{j=i-K+3}^{i-1} |\log S^i(t_j) - \log S^i(t_{j-1}) + O_p(\Delta t^{\frac{3}{2}-\delta+\alpha})| |\log S^i(t_{j-1}) - \log S^i(t_{j-2}) + O_p(\Delta t^{\frac{3}{2}-\delta+\alpha})| \\ &= \frac{1}{(K-2)\Delta t} \sum_{j=i-K+3}^{i-1} |\log S^i(t_j) - \log S^i(t_{j-1})| |\log S^i(t_{j-1}) - \log S^i(t_{j-2})| + O_p(\Delta t^{\frac{3}{2}-\delta+\alpha}) \\ &= \frac{1}{K-2} \sum_{j=i-K+3}^{i-1} \sigma^2(t_{i-K}) |\sqrt{\Delta t} U_j| |\sqrt{\Delta t} U_{j-1}| + O_p(\Delta t^{\frac{3}{2}-\delta+\alpha}) \\ &= \sigma^2(t_{i-K}) c^2 + O_p(\Delta t^{\frac{3}{2}-\delta+\alpha})\end{aligned}$$

where U_i 's are iid $Normal(0, 1)$ and $c = E(|U_i|) \approx 0.7979$. Then

$$T(t_i) = \frac{(U_i - \bar{U}_{i-1})}{c} + O_p(\Delta t^{\frac{3}{2}-\delta+\alpha})$$

This proves Theorem 1 and Theorem 1.1.

Alternatively, for the non-zero drift case, we can use Girsanov's Theorem to suppose $\mu(t) = 0$ as in Zhang, Mykland and Ait-Sahalia (2005).

6.3 Proof of Theorem 2

When there is a possibility of rare Poisson jumps in the window, the scaled bipower variation, $c^2 \hat{\sigma}^2(t)$ can be decomposed into two parts: one with jump terms and one without jump terms as

follows.

$$\begin{aligned}
c^2 \hat{\sigma}^2(t) &= \frac{1}{(K-2)\Delta t} \sum_{j=i-K+2}^{i-1} |\log S(t_j) - \log S(t_{j-1})| |\log S(t_{j-1}) - \log S(t_{j-2})| \\
&= \text{terms without jumps} + \frac{1}{(K-2)\Delta t} \sum_{\text{terms with jumps}} \sigma(t_j) |\Delta W_{t_j}| |Jump| \\
&= \text{terms without jumps} + \frac{1}{(K-2)\Delta t} O_p(\sqrt{\Delta t}) \sum_{\text{terms with jumps}} \sigma(t_j) |Jump| \\
&= \text{terms without jumps} + \frac{1}{(K-2)\Delta t} O_p(\sqrt{\Delta t})
\end{aligned}$$

The order of the second term is due to the property of the Poisson jump process that allows finite number of jumps over the window. Since $\sigma(t_j) |Jump| = O_p(1)$, $\sum_{\text{terms with jumps}} \sigma(t_j) |Jump| = O_p(1)$. The effect of jump terms becoming negligible requires the second term to be $o_p(1)$ as Δt goes to 0. The window size K that satisfies $K\sqrt{\Delta t} \rightarrow \infty$ and $K\Delta t \rightarrow 0$ as Δt goes to 0 will work. If we assume the window size to be $K = \beta\Delta t^\alpha$ where β is some constant, then the necessary condition for α is $-1 < \alpha < -0.5$. Accordingly,

$$\lim_{\Delta t \rightarrow 0} \hat{\sigma}^2|_{\text{alternative}} = \lim_{\Delta t \rightarrow 0} \hat{\sigma}^2|_{\text{null}} = \sigma^2(t).$$

Then putting the approximation for return above in the statistic yields

$$T(t_i) \approx \frac{\sigma_{t_{i-K}} \sqrt{\Delta t} U_i + Y(\tau) I_{\tau \in (t_{i-1}, t_i)}}{c \sigma(t_{i-K}) \sqrt{\Delta t}} = \frac{U_i}{c} + \frac{Y(\tau)}{c \sigma \sqrt{\Delta t}} I_{\tau \in (t_{i-1}, t_i)}$$

6.4 Proof of Lemma 1

It follows from Aldous (1985) and the proof in Galambos (1978).

6.5 Proof of Theorem 3

We suppose there are N jumps from time $t = 0$ to $t = T$ and claim there is a jump if $|T(t_i)| > \beta_n S_n + C_n$. Fix a set of jump times as $A_n = \{i : \text{there is a jump in } (t_{i-1}, t_i]\}$. Then

$$P(\text{We correctly classify all } N \text{ jumps} | N \text{ jumps}) = P(\text{For all } i \in A_n, |T(t_i)| > \beta_n S_n + C_n)$$

$$\begin{aligned}
&\approx \prod_{i \in A_n} P(|T(t_i)| > \beta_n S_n + C_n) \approx \prod_{i \in A_n} P(|Y(t_i)| > (\beta_n S_n + C_n) c \sigma \sqrt{\Delta t}) \\
&= \prod_{i \in A_n} \left(1 - F_{|Y|}(y_n)\right) \sim \left(1 - \frac{2}{\sqrt{2\pi}} y_n + o(y_n^2)\right)^N = 1 - \frac{2}{\sqrt{2\pi}} y_n N + o(y_n^2 N)
\end{aligned}$$

6.6 Proof of Theorem 4

Let $A_n^C = \{0, 1, \dots, n-1\} - A_n$ be a set of non-jump times. Then

$$\begin{aligned}
&P(\text{We incorrectly reject any non-jumps} | N \text{ jumps}) \\
&= P(\text{for some } i \in A_n^C, |T(t_i)| > \beta_n S_n + C_n | N \text{ jumps}) \\
&= P(\max_{i \in A_n^C} |T(t_i)| > \beta_n S_n + C_n | N \text{ jumps}) \\
&\approx P(\max_{i \in A_n^C} |\hat{T}(t_i)| > \beta_n S_n + C_n) = 1 - F_\xi(\beta_n) = \exp(-\beta_n) + o(\exp(-\beta_n)).
\end{aligned}$$

By L'Hopital's rule, we obtain the last step because

$$\lim_{\beta_n \rightarrow \infty} \frac{1 - F_\xi(\beta_n)}{\exp(-\beta_n)} = 1$$

7 References

- Aït-Sahalia, Y., 2002, "Telling from discrete data whether the underlying continuous-time model is a diffusion," *Journal of Finance* 57, 2075-2112
- Aït-Sahalia, Y., 2004, "Disentangling Diffusion from Jumps," *Journal of Financial Economics* 74, 487-528
- Aït-Sahalia, Y. and J. Jacod, 2005, "Fisher's Information for Discretely Sampled Levy Processes," Working Paper, Princeton University
- Aldous, D., 1989, "Probability Approximations via the Poisson Clumping Heuristic, Springer.
- Andersen, T. G., L. Benzoni, and J. Lund, 2002, "An empirical investigation of continuous-time equity return models," *Journal of Finance* 57, 1239-1284
- Bakshi, Cao, and Chen, 1997, "Empirical Performance of alternative Option Pricing Models," *Journal of Finance* 52, 2003-2049
- Bandi, F. M. and T. H. Nguyen, 2003, "On the functional estimation of jump-diffusion models," *Journal of Econometrics* 116, 293-328
- Barndorff-Nielsen, O. E., and N. Shephard, 2004, "Power and bipower variation with stochastic volatility and jumps," *Journal of Financial Econometrics* 2, 1-48
- Barndorff-Nielsen, O. E., and N. Shephard, 2004, "Econometrics of testing for jumps in financial economics using bipower variation," Working paper: Nuffield College, Oxford
- Bates, D. S., 1996, "Jumps and Stochastic Volatility: Exchange Rate Processes Implicit in Deutsch Mark Options," *Review of Financial Studies* 9, 69-107
- Bates, D. S., 2000, "Post-'87 Crash Fears in the S&P 500 Futures Option Market," *Journal of Econometrics* 94, 181-238
- Bertsimas, D., L. Kogan, and A. Lo, 2001, "Hedging Derivative Securities and Incomplete Mar-

- kets: An Epsilon-Arbitrage Approach,” *Operations Research* 49, 372-397
- Black, Fischer and Myron S. Scholes, 1973, “The pricing of options and corporate liabilities,” *Journal of Political Economy* 81, 637-654
- Chernov, M., A.R. Gallant, E. Ghysels, and G. Tauchen, 2003, “Alternative Models for Stock Price Dynamics,” *Journal of Econometrics* 116, 225-257
- Collin-Dufresne, P. and J. Hugonnier, 2001, “Event Risk, Contingent Claims and the Temporal Resolution of Uncertainty,” Working Paper, Carnegie Mellon University
- Collin-Dufresne, P. and J. Hugonnier, 2002, “Pricing and Hedging in the Presence of Extraneous Risks,” Working Paper, Carnegie Mellon University
- Cox, J. T., J. E. Ingersoll, and S. A. Ross, 1985, “A theory of the term structure of interest rates,” *Econometrica* 53, 385-407
- Duffie, D., 1995, *Dynamic Asset Pricing Theory*. 2nd Edition. Princeton University Press
- Duffie, D., J. Pan, and K. Singleton, 2000, “Transform analysis and asset pricing for affine jump diffusions,” *Econometrica* 68, 1343-1376
- Eraker, B., M. Johannes, N. Polson, 2003, “The Impact of Jumps in Volatility and Returns,” *Journal of Finance* 53, 1269-1300
- Galambos, J., 1978, *The Asymptotic Theory of Extreme Order Statistics*. John Wiley and Sons, Inc.
- Jacod, J. and A. N. Shriyaev, 1980, *Limit Theorems for stochastic processes*. Berlin New York: Springer
- Johannes, M., 2004, “The statistical and Economic Role of Jumps in Interest Rates,” *Journal of Finance* 59, 227-260
- Kloeden, P. E. and E. Platen, 1992, *Numerical Solution of Stochastic Differential Equations*.

Springer-Verlag

Kou, S. G., 2002, "A Jump Diffusion Model for Option Pricing," *Management Science* 48, 1086-1101

Lee, S. Y., 2004, "Jumps in Efficient Prices under Market Microstructure Noise," Working Paper, University of Chicago

Liu, J., F. Longstaff, and J. Pan, 2003, "Dynamic Asset Allocation with Event Risk," *Journal of Finance* 58, 231-259

Maheu, J. M. and T. H. McCurdy, 2004, "New Arrival, Jump Dynamics, and Volatility Components for Individual Stock Returns," *Journal of Finance* 59, 755-793

Merton, R. C., 1976, "Option Pricing when Underlying Stock Returns are Discontinuous," *Journal of Financial Economics* 3, 125-144

Merton, R. C., 1990, Continuous-time Finance. Blackwell, Cambridge

Mykland, P. and L. Zhang, 2001, "Anova for diffusions," Technical Report 507, Department of Statistics, University of Chicago

Pan, J., 2002, "The Jump-Risk Premia Implicit in Options: Evidence from an Integrated Time-Series Study," *Journal of Financial Economics* 63, 3-50

Piazzesi, M., 2003, "Bond yields and the Federal Reserve," *Journal of Political Economy* 113, 311-344.

Pollard, D., 2001, A User's Guide of Measure Theoretic Probability. Cambridge University Press.

Protter, Philip, 1995, Stochastic Integration and Differential Equations: A New Approach. Berlin New York: Springer

Schaumburg, E., 2001, "Maximum Likelihood Estimation of Jump Processes with Applications to Finance," Ph.D. Dissertation, Princeton University

Tsay, Ruey S., 2001, A Manuscript, Chapter 10. Markov Chain Monte Carlo Methods with Applications

List of Footnotes

1. See Bates (2000), and Bakshi *et al.* (1997) and the reference therein.
2. See Liu *et al.* (2003), Eraker *et al.* (2003), Naik and Lee (1990), Duffie *et al.* (2000), and Piazzesi (2003).
3. Maheu and McCurdy (2003) studies the new arrival and dynamic feature of jumps in individual stock markets.
4. Note that in the literature on implied binomial tree for option pricing, the term “local volatility” is used in a different manner.

List of Tables

I	The mean and standard error (in parenthesis) of the size of the test when the significance level α is 5%. The null model is a diffusion process with fixed volatilities, σ at 30% and 60%. NOBS denotes the number of observations per day.	15
II	The mean and standard error (in parenthesis) of power of the test when the significance level α is 5%. The null model is a diffusion process with fixed volatility σ at 30% and jump size $y \times \sigma$. NOBS denotes the number of observations per day.	17
III	The mean and standard error (in parenthesis) of the size of the test when the significance level α is 5%. The null model is a diffusion process with stochastic volatility. NOBS denotes the number of observations per day.	19
IV	The mean and standard error (in parenthesis) of the power of the test when the significance level α is 5%. The null model is a diffusion process with stochastic volatility and the jump size depends on the mean of volatility $\widetilde{\sigma(t)} = E[\sigma(t)]$ with $y \times \widetilde{\sigma(t)}$	20
V	The parameter estimates for the autoregressive jump arrival model. The significance level of each test is set at $100 \times \alpha\%$, which classifies the detected jump sizes.	22
VI	The parameter estimates for the autoregressive jump arrival model. The significance level of each test is set at $100 \times \alpha\%$, which classifies the detected jump sizes.	23
VII	The examples of 99%-VaR of currency exchange rate and its options. Values of VaR are in percentages. The underlying exchange rate of return process has volatility at 30%, standard deviation of jump size distribution at 60%, fixed jump intensity at 10 per a year. The β_1 coefficient is at 5%.	25
VIII	Mean Squared Error 1: $Err_1 = \hat{\Lambda}(T) - \Lambda^{actual}(T)$	27
IX	Mean Squared Errors for 6 hourly data with $T = 1, 3, 5, 7, 10$	28

List of Figures

1	Formation of our new test with a window size $K = 10$	8
2	Sample return series simulated from a jump diffusion with constant volatility at 30% and real return of Japanese Yen against United States Dollar and German Mark against United States Dollar	16
3	Graphs of Mean Squared Total Error with daily and 6 hourly data as a function of window size K	28